Synthesis and Characterization of New Segmented Copolymers with Side Chain Liquid Crystalline Soft Segments

Bindu R. Nair, Marlon A. R. Osbourne, and Paula T. Hammond*

Department of Chemical Engineering, Massachusetts Institute of Technology, Cambridge, Massachusetts 02139

Received May 12, 1998; Revised Manuscript Received September 25, 1998

ABSTRACT: Liquid crystalline polyurethane thermoplastic elastomers with cyano−biphenyl mesogens pendant on the soft segment have been synthesized for the first time. These materials offer a unique opportunity to study the interplay between the liquid crystalline ordering of the elastomer and the morphology of the segmented copolymer. We present the synthesis of carbinol end-capped hydromethylsiloxane oligomers, which can be functionalized with mesogen via a hydrosilylation technique. These side chain liquid crystalline (LC) siloxane macromonomers are then converted to segmented polyurethanes using traditional urethane chemistry. Structural analysis and characterization of the resulting polymers is provided, along with a comparison study of the thermal and optical behavior of these urethanes as the spacer length is increased from 3 to 8 methylene units. Polymers with a high degree of decoupling (spacer length = 8) are above the soft segment T_g at room temperature with a stablized smectic phase. Less decoupled polymers (spacer length = 3) are harder, flaky materials which exhibit a nematic phase at high temperatures. Discussions of the effects of the hard segment mobility on the phase behavior of these liquid crystalline polyurethanes is offered. These materials show promise as elastomers with mechanooptic and electrooptic behavior.

Introduction

Side chain liquid crystalline polymers couple the behavior of liquid crystals and classical polymeric materials. Advantages of these systems include the inherent film forming properties of polymers and the enhanced mechanical stability that polymers can provide. Much work has been done on the phase behavior as well as the electrooptical response of side chain liquid crystalline polymers; however, because linear liquid crystalline polymers are fluid in the liquid crystalline (LC) state, they do not exhibit cohesive mechanical properties. The coupling of mesogens to a polymer network allows the exploration of optical responses to mechanical fields.[1,2] The first side chain LC elastomers were synthesized by Finkelmann and co-workers.[3] These materials exhibited a number of interesting mechanooptical effects, including changes in light transmittance with mechanical strain. The incorporation of ferroelectric mesogens in such networks resulted in the observation of second harmonic generation[4] and piezoelectric effects.[5−8] Liquid crystalline monodomains have been obtained by mechanical orientation of lightly cross-linked networks, followed by further cross-linking.[9,10] However, these polymers are covalently cross-linked; therefore, the mobility of the liquid crystalline units is impeded by the chemical cross-links, and the observation of electrooptical switching[11] and piezoelectric behavior[8] is decreased as the cross-link density is increased. Another limitation of all cross-linked systems is the relatively limited processing and orientation techniques possible for thermoset materials and the irreversible nature of chemical cross-linking.

A solution to these issues is the use of thermoplastic elastomers with liquid crystalline segments. In addition to potentially minimizing the loss of mobility afforded by the presence of covalent cross-link units, thermoplastic elastomers offer a host of opportunities to control the morphology of the polymer. Liquid crystalline orientation can be altered by processing, and "frozen" into a sample below the flow temperature of the polymer. The behavior of liquid crystals in this morphologically rich environment should provide further insights into the mechanooptic behavior of liquid crystalline polymers. This paper reports the synthesis and initial characterization of a new class of side chain liquid crystalline polyurethanes. Although many traditional polyurethanes have been made with liquid crystalline hard segments[12,13] or chain extenders,[14,15] none have been designed to exhibit electro- or mechanoresponsive elastomeric properties via functionalization of the flexible soft segments or blocks. We present for the first time a polyurethane with liquid crystals pendant to the soft segment to be studied for mechanooptic applications.

Experimental Section

Materials. Mesogen. Potassium hydroxide, 4′-hydroxy-4-biphenylcarbonitrile, 3-bromo-1-propene, 8-bromo-1-octene, and 6-bromo-1-hexene were used as bought from Aldrich.

Soft Segment. Acetoxyethyldimethylchlorosilane and dichloromethylsilane were used as bought from Gelest and handled under nitrogen. Hexachloroplatinic acid (99+%) was used as bought from Aldrich. For both the mesogen and the siloxane, solvents were used as bought from VWR.

Polyurethane. 4,4′-Methylenebis(phenylisocyanate) (MDI) and 1,4-butanediol were vacuum distilled and then stored under nitrogen for no more than 3 days prior to use. Anhydrous dimethylacetamide (DMAc) was used as bought from Aldrich under nitrogen. Tetrahydrofuran (THF) was distilled over CaH_2 just prior to use.

Synthesis. Three different polyurethanes with different length alkyl spacers were synthesized. The mesogen is a cyano−biphenyl mesogen (**1**).

$$H_2C=CH-(CH_2)_{\overline{n-2}}O-\bigcirc\!\!-\bigcirc\!\!-CN$$

1
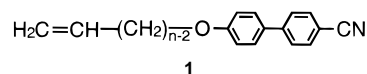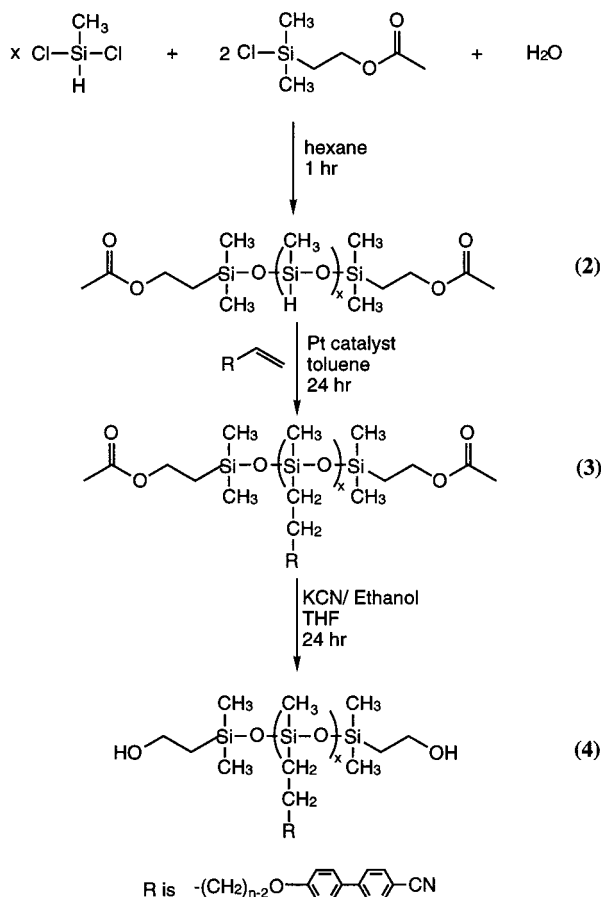
Figure 1. Synthesis of soft segment macrodiol.

The polyurethanes were synthesized with spacers of three, six, and eight methylene units and are called U3, U6, and U8, respectively. The siloxane macrodiols from which they were synthesized are denoted S3, S6, and S8 whereas the low molar mass vinyl mesogens are called M3, M6, and M8, respectively. Since the same synthetic technique is used for all three polyurethanes, only the steps for U3 are reported here.

Mesogen 1.[16] A 0.055 mol sample of KOH pellets in 10 mL of water is added to 0.05 mol of 4′-hydroxy-4-biphenylcarbonitrile in 90 mL of ethanol and refluxed for 15 min. Then 0.05 mol 3-bromo-1-propene is added and the reaction allowed to reflux overnight. The reaction mixture is neutralized with HCl and then poured into a separation funnel with 300 mL of CH_2Cl_2 and 200 mL of water. The organic phase is dried over anhydrous $MgSO_4$ and then concentrated. The pure product (**1**) is recrystallized from methanol at a yield of 70%.

NMR of mesogen **1** in $CDCl_3$: CH_2=CH− (quadruplet δ 5.34, 5.36, 5.45, 5.49); CH_2=CH− (multiplet δ 6.15); phenyl rings (several peaks δ between 7.03 and 7.73); various CH_2 peaks; CH_2−O−Ph (δ 4.63 and 4.01 depending on n = 3, 6, or 8).

Soft Segment 4. The soft segment is a polysiloxane with pendant liquid crystalline moieties end-capped with carbinol groups (**4**) and is synthesized as shown in Figure 1. Hydromethylsiloxane **2** is made by a polycondensation process. First 10 g (0.0869 mol) of dichloromethylsilane and a premeasured amount of acetoxyethyldimethylchlorosilane (depending on desired molecular weight) are transferred under nitrogen into an addition funnel. Water is placed in a round-bottom flask such that the reaction produces a 20% HCl solution. The contents of the addition funnel are diluted with hexane and then added to the water over the course of 5 min. The exothermic reaction occurs immediately, but the reaction mixture is allowed to stir for 1 h until the reaction vessel is no longer warm. The contents of the reaction mixture are poured into a separation funnel with 50−100 mL each of water and hexane. The organic phase is concentrated at 40 °C under

reduced pressure and then dried on a vacuum line at 45 °C for 24 h to remove any cyclics.

NMR of hydromethylsiloxane **2** in $CDCl_3$: Si−H (δ 4.73); Si−CH$_2$CH_2−OC(O)CH$_3$ (triplet δ 4.23, 4.21, 4.19); OC(O)CH_3 (δ 2.05); Si−CH$_2$ (triplet δ 1.07, 1.09, 1.11); Si−CH$_3$ (δ between 0.14 and 0.22).

The next step in the reaction sequence is to make the substituted siloxane (**3**). Hydromethylsiloxane **2** and a 10% excess of vinyl mesogen **1** are reacted for 24 h at 40−50 °C with 2 drops of hexachloroplatinic acid (0.12 M in THF) in toluene. The reaction is monitored using FTIR and allowed to proceed until the disappearance of the Si−H vibration (2164 cm^{-1}) is complete. This reaction mixture is concentrated and purified by column chromatography (eluent: CH_2Cl_2 to wash off excess mesogen followed by THF to remove from column). GPC as well as thin-layer chromatography of this substituted siloxane indicates no traces of unattached mesogen.

NMR of substituted siloxane **3** in $CDCl_3$: Combination of **1** and **2**; disappearance of vinyl peaks (quadruplet and multiplet); disappearance of Si−H. All other peaks were broadened.

Finally, the substituted siloxane (**3**) is deprotected to reveal carbinol end groups (**4**) using a mild transesterification process.[17] The acetoxy end-capped siloxane recovered from the column is dissolved in 20 mL of tetrahydrofuran. Then 0.4 g of KCN is dissolved in 2 mL of H_2O and 19 mL of ethanol is added to the aqueous KCN. This solution is added to the THF solution and THF is added until all components dissolve. The reaction mixture is refluxed for 2 days and the disappearance of the carbonyl peak (1736 cm^{-1}) is monitored by FTIR. The reaction mixture is then concentrated and contacted with water several times to remove KCN impurities and then dried under vacuum for several days to remove any excess water.

NMR of deprotected siloxane **4** in $CDCl_3$: Same as for **3** except for the disappearance of CH_2OAc and −OC(O)CH_3 (triplet and singlet). −OH peak was not visible.

Polyurethane 5. The polyurethane (**5**) is made using a two-step process described in Figure 2. All glassware is flame-dried prior to use and this reaction is kept under nitrogen at all times to reduce side reactions with water. A solution of siloxane **4** in a 50/50 mixture of DMAc and THF is prepared in an addition funnel. A 2× molar excess of MDI is measured into the reaction flask and the siloxane solution is added over the course of 1 h into the reaction vessel. The reaction is allowed to proceed for 3 h, after which FTIR is done to verify the creation of urethane bonds (1728 cm^{-1}). Then 1 mol equiv of butanediol is syringed into the reaction mixture and the reaction allowed to proceed overnight. The final product (**5**) is isolated by precipitation from methanol.

Urethane **5** in 50/50 CDCl$_3$/ DMSO (deuterated): All peaks in **4** and Ph-N(H)C(O)O (δ 8.10), and CH_2−OC(O)N(H) (δ 3.90).

Characterization. Chemical structure of the polyurethanes and all chemical intermediates were confirmed using ^{1}H NMR performed on a Bruker Avance DPX-400 and FTIR with a Nicolet Magna-IR 550 Series II spectrometer using a DTGS KBr detector on 3M Teflon IR cards.

Molecular weights of polysiloxane polymers were determined using Gel Permeation Chromatography (GPC) on all relevant samples using a Waters system and ultraviolet detectors. Intrinsic viscosity measurements were made on segmented polyurethanes using an OC Ubbeholde viscometer in a Polyscience constant-temperature water bath.

Thermal phase behavior was studied with differential scanning calorimetry (DSC) using a Perkin-Elmer DSC 7 AMB. Transitions were verified using optical microscopy on a Kramer Scientific Leitz DMRX microscope in transmission. Room-temperature small angle X-ray scattering (SAXS) experiments were performed on a Siemens small angle scattering diffractometer with a Rigaku 18W rotating anode X-ray generator. SAXS patterns at elevated temperatures necessitated the use of an Instec RTC-1 temperature controller. Samples were prepared by casting a thin film from a 50/50 solution of DMAc/ THF.
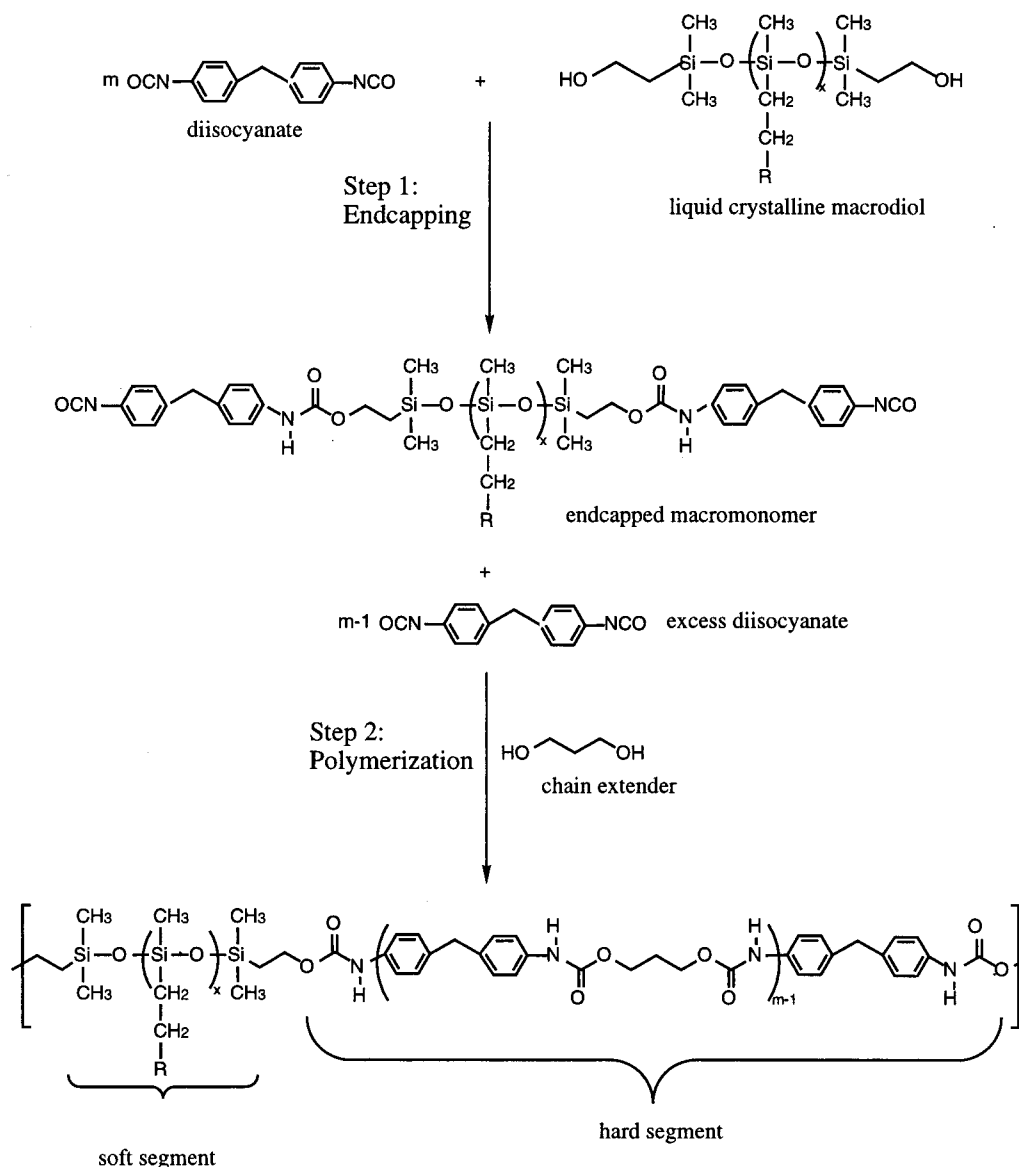
Figure 2. Two-step polyurethane synthesis.

Results and Discussion

Design and Synthesis. Figure 2 shows the structure of the desired polymer. This material is designed to provide a phase segregated morphology such that the pendant liquid crystalline groups in the soft segment are free to respond to applied fields while anchored by the hard domains. A siloxane backbone is used in the soft segment because siloxanes are known to be very low glass transition (T_g) materials. Nonsubstituted hydromethylsiloxanes have T_gs on the order of -110 °C. Siloxane oligomers substituted with the cyano−biphenyl mesogens of the type reported in this paper have been shown to have T_gs between -16 and 25 °C depending on the length of the spacer group.[18]
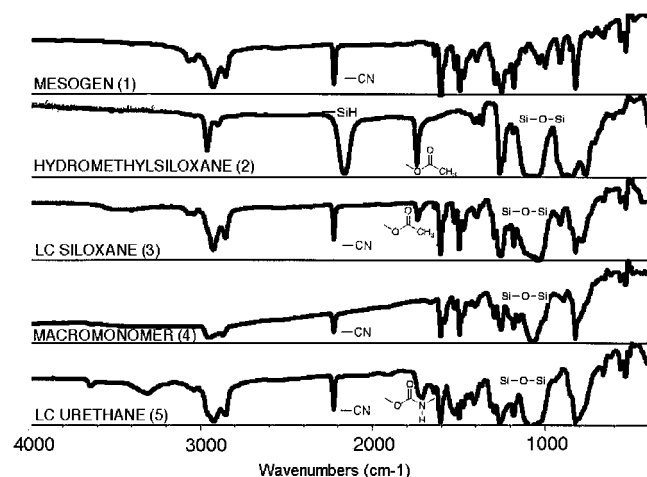
The choice of the cyano−biphenyl mesogen is governed by the well characterized nature of this mesogen, and the fact that the cyano group is known to induce nematic LC behavior. The relative stability of the nematic versus smectic phase is governed by the length of the alkyl spacer, which favors smectic phases as its length increases. Another advantage of the mesogen is the clear signature that the cyano group affords in FT-IR. This IR tag will allow us to perform IR dichroism studies to understand the orientation of the mesogen on the application of a stress field.[2]

The cyano−biphenyl mesogen is synthesized using well documented Williamson ether techniques,[16] and then attached to polysiloxane oligomers using a traditional hydrosilylation step. Our challenge in synthesizing the segmented polyurethanes was in acquiring hydromethyl siloxane oligomers that were end functionalized with carbinol groups. The three-step approach shown in Figure 1 was found to be most effective in obtaining these functional siloxanes.

Polyurethanes have previously been made with poly-(dimethylsiloxane) oligomers end-capped with carbinol groups. The synthesis of these dimethylsiloxanes without the base and heat-sensitive Si−H groups has been reported widely in the literature. Hydromethylsiloxanes end-capped with silanol groups can be readily synthesized or purchased. However, a hydromethylsiloxane end-capped with carbinol groups has not been previously reported in the literature. Anionic polymerization is not feasible due to the reactivity of the Si−H groups. Cationic polymerization of a cyclic tetramer and appropriate endcapping agent produces polymers of a large

Figure 3. FT-IR of reaction sequence. (1) mesogen; (2) hydromethylsiloxane; (3) substituted siloxane; (4) deprotected siloxane; (5) urethane.

Table 1. Thermal Phase Behavior of Polyurethanes and Precursor Materials

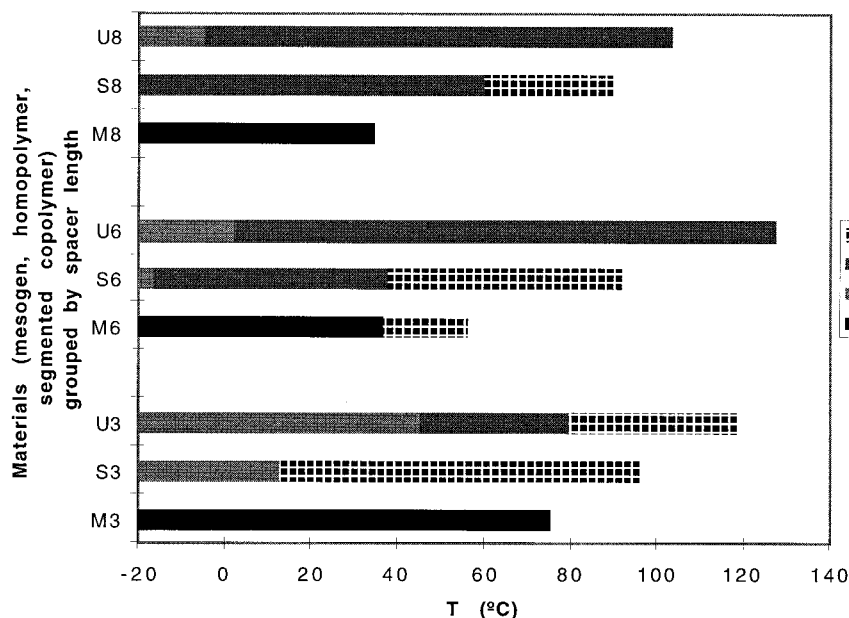| material	T_g (°C)	T_{exo} (°C)	T_m (°C)	T_{s-n} (°C) [ΔH (J/g)]	T_{lc-i} (°C) [ΔH (J/g)]
M3			76		
S3	13				96
U3	45[a]			79.8 [8.007]	118.9 [0.076]
M6			36.8		56.5
S6	−16			38	92
U6	2.3, 163				125.6 [5.618]
M8			35		
S8	<−20			60	90
U8	−4.7, 88	55.7			104.2 [4.329]

[a] Estimated by observing when material softens using a hot stage. Transition not clear in DSC.

Polymer Characterization. Due to the heterogeneous nature of segmented copolymers, and the large differences in polarity between the urethane and siloxane segments, the polyurethanes are only soluble in a limited number of solvent mixtures. The siloxane block is generally soluble in less polar solvents such as toluene or THF, whereas polyurethanes are generally soluble in polar and H-bonding solvents. The best solvents for the polyurethane copolymers are 50/50 mixtures of DMAc/THF and CH_2Cl_2/DMSO. Films could be cast from these solvent mixtures to produce free-standing films with a cloudy or opaque appearance due to the presence of the liquid crystalline phase.

The molecular weight distribution of the siloxanes was analyzed with conventional techniques such as gel permeation chromatography (GPC). The hydromethylsiloxane **(2)** was analyzed using proton NMR. The ratio of the endgroups to the Si–H groups provided an estimate of the degree of polymerization of the siloxane chain, which ranged from 16 to 24 Si–O repeat units. Upon addition of the mesogen, a GPC of the material in THF was run to corroborate the NMR predictions as well as to verify the removal of all cyclics and excess mesogen. The polydispersity index (PDI) of these materials ranged from 1.5 to 1.7.

GPC could not be performed on the urethanes because they are not soluble in THF or any one solvent. Therefore, the size of these molecules was estimated using intrinsic viscosity measurements in a 50/50 DMAc/THF mixture at 40 °C. The U8 sample was found to have an intrinsic viscosity of 0.4 dL/g and U3 had an intrinsic viscosity of 0.5 dL/g. These numbers suggest that the polyurethanes prepared are of relatively low molecular weight. Preliminary measurements of the intrinsic viscosity for the more recently synthesized U6 polyurethane indicates a value of about 0.6 dL/g; the mechanical integrity of the U6 films also suggests a higher molecular weight material. Previous literature has reported the use of intrinsic viscosity to measure the molecular size of siloxane polyurethanes in similar solvent mixtures at 40 °C;[14] polymers with viscosities of 0.4 dL/g were described as "low" molecular weight polyurethanes, whereas 0.8 dL/g intrinsic viscosities were considered "high" molecular weight.

Morphological and Thermal Phase Behavior. Both liquid crystalline and polymer phase transitions of the three polyurethanes and their precursors are shown in Table 1. A graphical depiction of the same data can be found in Figure 4. Phase behavior and transition temperatures were determined using differential scanning calorimetry (DSC), polarizing optical microscopy, and X-ray scattering.

polydispersity index as well as the formation of many cyclics. In the approach outlined in Figure 1, a dichlorohydromethylsilane was polymerized using step polycondensation. This approach gives us some control over molecular weight and polydispersity. The step polymerization works best if enough water is added such that a 20% HCl solution exists at the end of the polymerization. This acid content shifts the chain/ring equilibrium such that about 30% of the monomer ends up as rings. These rings can be removed by vacuum-drying.

The endcapping agent used is an acetoxyethyldimethylchlorosilane. Since a molecule with a Si–Cl group is unstable in the presence of a carbinol group, it was necessary to endcap with a functional group that could be quantitatively converted to an alcohol. The acetoxyterminated siloxane **(2)** has to be deprotected using mild conditions such that the base-sensitive siloxane will not depolymerize into cycles. These criteria led to the choice of KCN as the catalyst for the ester interchange reaction that would deprotect the acetoxy group.[17] The Si–H group is heat sensitive and can cross-link at high temperatures if there is any base present; therefore, we substitute the mesogen prior to the deprotection of the alcohol. The final step of the process is the synthesis of the polyurethane using the classical two-step process shown in Figure 2.

The chemical structure was identified, and the progress of the reactions was monitored primarily by use of FTIR spectroscopy. ^{1}H NMR was used to verify the conclusions drawn from IR analysis for all samples and these data is presented in the Experimental Section. Figure 3 shows FTIR taken at various points during the siloxane functionalization and polyurethane synthesis. The appearance and disappearance of key vibrations are labeled and can be seen clearly. The hydromethylsiloxane **(2)** shows a strong Si–H vibration (2164 cm^{-1}) and a carbonyl ester vibration (1743 cm^{-1}) from the endcapped acetoxy groups. Upon addition of the mesogen **(1)**, the –CN (2225 cm^{-1}) vibration appears. The acetoxy group in the substituted siloxane **(3)** appears at lower wavenumbers (1736 cm^{-1}) than its unsubstituted counterpart **(2)**; this shift can be attributed to the loss of carbonyl H-bonding with Si–H groups. The deprotection shows the disappearance of the carbonyl peak associated with the end-capped acetoxy group. Finally, the appearance of the urethane carbonyl (1728 cm^{-1}) can be seen in the IR spectra of the polyurethane **(5)**.

Figure 4. Graphical depiction of phase behavior shown in Table 1 indicating stablization of smectic phase in LCPUs.

The polyurethanes exhibit varying degrees of phase segregation as indicated by DSC and SAXS. The polyurethane with the shortest spacer, U3, appears somewhat phase mixed as indicated by the high T_g of this material and the fact that we do not observe a T_g for the second block in DSC. The T_g reported in Table 1 for U3 is an estimate of the temperature at which the polyurethane undergoes a softening point. Room-temperature SAXS indicates no sign of phase segregated domains in the U3 material. The longer alkyl spacer polyurethanes, U6 and U8, both show signs of phase segregation. The U8 polyurethane has two glass transitions that can be seen clearly in DSC as reported in Table 1. The soft segment undergoes a softening transition at −4.6 °C while the hard segment has a glass transition that appears at 88 °C. The glass transition of the siloxane homopolymer, S8, is lower than −20 °C; thus, the glass transition is increased considerably on incorporation of the soft segment into the polyurethane, suggesting that the system is partially phase mixed. Despite the indication of phase ordering from the DSC data, the U8 material does not exhibit a detectable peak in SAXS diffractograms corresponding to hard segment domains. The U6 polyurethane appears to be a more highly phase segregated system. The T_gs of both component segments are detectable in the DSC. The siloxane homopolymer, S6, has a T_g of −16 °C which is raised slightly upon incorporation into the urethane U6 to 2.3 °C; additionally, the MDI transition at 163 °C is much higher in this material as compared to the U8. SAXS data also shows that this material is phase segregated. The diffractogram in Figure 5 indicates two types of spacings including the hard domain size of 65.4 Å due to phase segregation of the hard segments, as well as the smectic layer spacing.

As indicated by the U6 and U8 materials, the glass transition temperatures of the siloxane segments are increased when incorporated into the polyurethane. This observation is due in part to some degree of phase mixing, as well as a lowering of the segmental mobility of the LC polymer due to the formation of a microphase segregated network. Another anticipated result was a decrease in the soft segment glass transition temperature upon increasing the length of the alkyl spacer. The
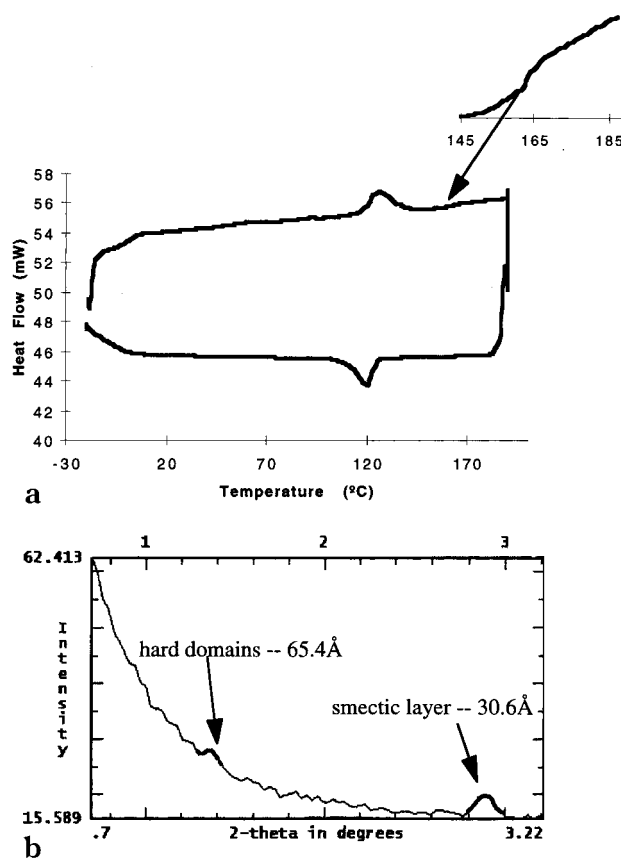
Figure 5. (a) DSC trace of U6 (10 °C/min); (b) SAXS of U6.

extent of decoupling between the mesogen and the backbone allows the polymer to retain its flexibility more effectively. We see this effect manifest in the physical nature of the polyurethanes. All three polyurethane materials were good film-forming polymers; however, films of the U3 material were hard and somewhat glassy at room temperature and pastelike at higher temperatures, whereas the U6 and U8 polymers formed tacky, somewhat rubbery, gums at room temperature.

Table 2. Smectic Layer Spacings of Polyurethanes as Determined by SAXS

Spacer Length	U3 (at 70°C)	U6	U8
Experimental Layer Spacing (Å)	16.3	30.6	36.8
Theoretical Layer Spacing (Å)	17.6	36.4	41.2
Proposed Layer Structure			

One of the most notable trends seen in Figure 4 is the expected stabilization of the liquid crystalline phase on incorporation of the mesogen onto a siloxane backbone, followed by a further stabilization upon incorporation of the siloxane in the polyurethane segmented copolymer. The cyano—biphenyl mesogens of spacer lengths 3 and 8 both show a single clear melting endotherm on heating; M6, the six spacer length mesogen, shows both a melting transition and an LC isotropization point. The appearance of or increased thermal stability of the LC phase in substituted siloxanes is consistent with previously reported liquid crystalline thermal transitions for LC side group polymers.[18] When the LC siloxane is incorporated into the polyurethane, the clearing point is further increased, indicating a greater stabilization of the liquid crystalline phase. This may be due in part to favorable interactions between the hard domain interface and the liquid crystalline phase. Liquid crystalline phases are known to be further stabilized at surfaces, and anchoring effects may be manifest in a multisegmented copolymer; similar observations have been made for liquid crystalline diblock copolymers.[19] Additionally, the presence of a hydrogen-bonded system may also increase the stability of the LC phase.

We also find in Table 1 and Figure 4 that the incorporation of the siloxane into the polyurethane favors stabilization of the smectic rather than the nematic phase. For example, the S3 material is nematic over its entire liquid crystalline range, but the U3 material undergoes a smectic to nematic transition near 80 °C. When the spacer length is increased in U6, the urethane loses all nematic character, and the smectic phase is fully stabilized. S6 shows a smectic to nematic transition at 38 °C but urethane U6 is smectic over the entire LC temperature range. The U8 material similarly shows stabilization of the smectic phase. The exotherm reported in U8 near 56 °C is reproducible on multiple heatings. It may be the result of cold crystallization [12] of the polyurethane hard segments. On the other hand, the exotherm is near the temperature of the original smectic—nematic transition in the precursor siloxane. This exotherm may be caused by a smectic phase reordering induced by suppression of the smectic—nematic phase change due to the presence of the polyurethane hard segments.

The smectic phase is verified by optical microscopy as discussed in the next section as well as by X-ray diffraction. Smectic layer spacings as determined by SAXS can be found in Table 2. The theoretical layer spacings listed in Table 2 are based on simple bond angle and bond length calculations for these mesogens assuming an all-trans configuration of the spacer groups. Both polyurethanes U6 and U8 show clear smectic layers at room temperature. These spacings indicate either bilayer or interdigitated layer structures of the

mesogens as illustrated in the table. The measured spacings are consistently lower than the theoretical spacings. This observation may be due to the flexible nature of the alkyl chains, which may assume conformations other than all-trans. A second possiblity for the U6 and U8 polymers is interdigitation between the smectic layers. A smectic layer peak is not detected in the U3 polyurethane at room temperature; this material is still in the glassy state at this temperature, and does not appear to exhibit any frozen-in smectic ordering at 25 °C. However, a diffratogram acquired at 70 °C, a temperature well above the T_g but within the range of the smectic phase, as seen in Figure 4, shows a clear smectic peak at 16.3 Å. This spacing agrees well with a single smectic layer as shown in Table 2. The smectic phase is also evidenced by optical microscopy and is described further in the following section.

The marked difference between the LC phase behavior of the U3 polymer and longer spacer length polymers is typical of small molecule LCs, for which longer alkyl spacers stabilize smectic phases over nematic phases. Under optical microscopy the difference in mobility between U3 and U8 is clear, especially at high temperatures. The smectic polymer U8 behaves in a sluggish manner that suggests the higher viscosities associated with smectic phases. The polymer with a nematic range has substantially more mobility associated with it.

Optical Microscopy. The DSC data is consistent with observations from optical microscopy between crossed polarizers. Optical microscopy was performed on pre-rubbed cells in which the cells were rubbed to induce planar orientation; cell thicknesses of 4 and 50 μm were used.

In the U8 polyurethane, the cell type did not significantly affect the phase transitions. On heating at 10 °C/min, all birefringence disappeared at 125 °C. The higher clearing temperature seen in the thin film cell as compared to the DSC transition reported in Table 1 could be explained by surface induced orientational order.[20] When the film was cooled after annealing in the isotropic melt for a few hours, needlelike batonnet structures started forming at 105 °C. These needles coalesced, and focal conic fans appeared as the sample was cooled. This batonnet to fan transition is classic smectic A behavior.[21] Figure 6 shows the images recorded while cooling the U8 polymer after annealing.

The U3 polymer exhibits optical behavior on cooling that is highly dependent on the size of the cell and consequently the film thickness. On heating, the samples in both the thinner and thicker cells exhibit a phase change at 75 °C indicated by a change in texture; a clearing point of 130 °C can also be observed. However, on cooling the two different cells have unique behavior patterns. In the thinner cell, birefringence first appears at 118 °C while the thicker cell shows this behavior at 122 °C. The classic nematic threaded structure shown in Figure 7a can be seen in both cases. This difference in the nematic—isotropic temperature (T_{N-I}) may be due to the varying surface or anchoring energies in the different polymer film surface treatments.

The phase change that occurs at 79 °C on cooling in the DSC trace of U3 is marked by an interesting change in optical texture. This transition results in chevron patterns that form as shown in Figures 7b and 8. This chevron pattern is often seen in nematic-smectic transitions.[22] During this transition, the image under the optical microscope undergoes a type of freezing behavior
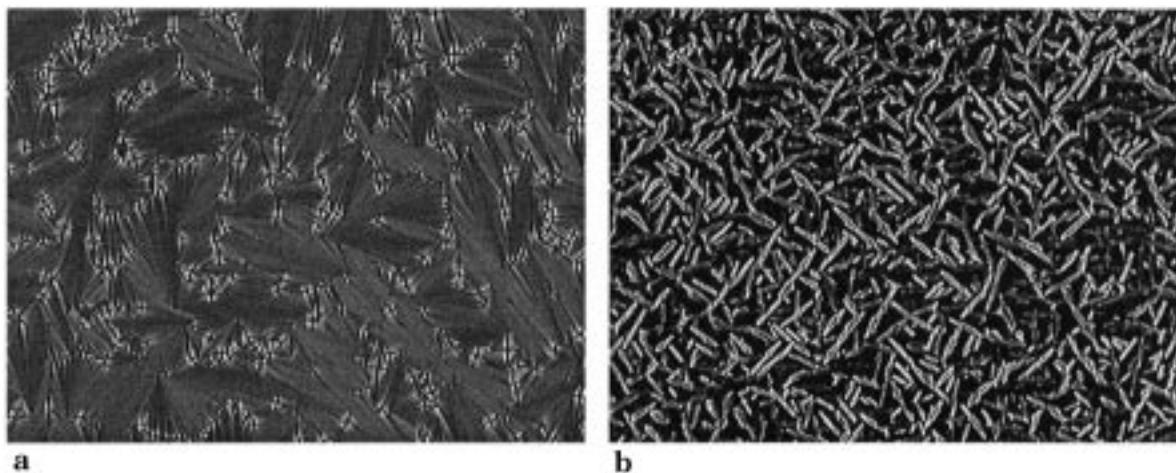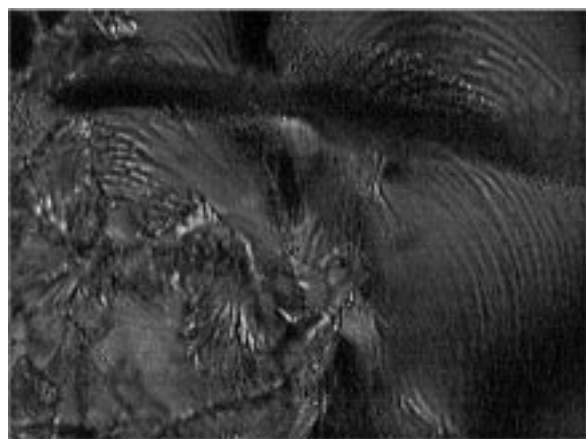
Figure 6. Optical micrographs of LCPU U8 between crossed polarizers on cooling after annealing in a 4 μm cell (a) 30 °C, 400×; (b) 100 °C, 200×.
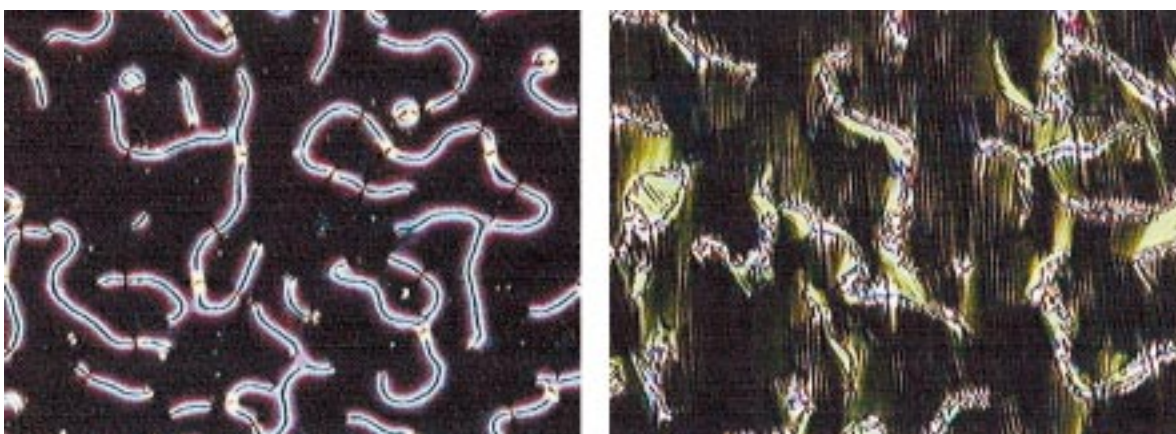
Figure 7. Optical micrographs of LCPU U3 between crossed polarizers on cooling after annealing in a 4 μm cell (a) 114 °C, 400×; (b) 95 °C, 400×.

Figure 8. Chevron patterns that appear at 75 °C in LCPU U3 in a 50 μm cell.

in which the sample loses much of its mobility. The optical texture then remains unchanged down to room temperature. This phase change appears to be associated with the introduction of the smectic phase and may also be affiliated with association of the hard segments. The corresponding smectic–nematic ($T_{\text{S–N}}$) endotherm observed in DSC heating is a single broad peak with an unusually large enthalpy (see Table 1). It is possible that this peak is a convolution of two or more transitions, based on the size and breadth of the transition. Although phase ordering was not detected from SAXS

and DSC, it may be possible that there is also a hard segment order–disorder process that is occurring in this temperature regime or that phase-mixed hard segments become incorporated into the smectic layers.

In the 50 μm cell, this phase change appears at 75 °C, which is consistent with the DSC data. However, in the 4 μm cell, the transition appears much earlier, at 95 °C. It is possible that the MDI segments of the polyurethane are inducing this phase change, as the MDI segments begin to hydrogen bond with functional groups on the rubbed polyimide surface, and align in the LC cell. In the thicker cell, the polymer is subject to more bulk behavior, and therefore, the transition temperature is closer to that found from DSC.

The coupling of polymer phase behavior and liquid crystalline transition behavior has also been observed in liquid crystalline block copolymers, for which microphase segregation and morphological effects can be influenced by the presence of the liquid crystalline phase.[19,23] In the case of polyurethanes, the scale of microphase segregation is much smaller; consequently, large interfacial areas can enhance the interrelationships between LC thermal transitions and polymer phase behavior. Even in the limit of fully phase mixed copolymers, the role of hard segments in inducing smectic ordering must be considered, as the length scale of the MDI hard segment for these materials approaches that of the cyanobiphenyl mesogen. The nature of this transition will be further explored.

Conclusions

Side chain liquid crystalline polyurethanes with the mesogenic groups directly attached to the soft segment have been synthesized for the first time. The complete synthetic technique as well as the structural characterization of cyano−biphenyl liquid crystalline polyurethanes with spacers of three, six, and eight methylene units is presented. These materials exhibit liquid crystalline phase behavior over broad temperature ranges. Thermal behavior of the polyurethanes is highly dependent on the length of the alkyl spacer. A smectic phase was found for the six and eight methyl spacer polyurethane, and a nematic material was obtained at high temperatures for the three spacer material. Also, liquid crystallinity was observed at room temperature for both the U6 and the U8 polymer, which were rubbery gums at 25EC. The U3 material exhibited a phase transition corresponding to a solidification of the polyurethane at high temperatures. This process is the result of the introduction of a smectic phase, induced by the presence of the hard segment. The nematic to smectic transition temperature is highly dependent on the thickness of the LC cell and occurs at higher temperatures in a thin cell on cooling. It is postulated that this effect is due to the relative importance of surface interactions of the polyurethane within the cell.

Initial observations of the thermal behavior in these new polyurethane systems suggest that an interplay between the liquid crystalline phase behavior and the segmented copolymer morphology will greatly influence the thermal and optical behavior of these polymers. These materials show promise as thermoplastic liquid crystalline elastomers with interesting mechano- and electrooptical properties. Future investigations include an investigation of orientation of liquid crystals with mechanical stress and the synthesis of higher molecular weight polymers with increased mechanical integrity and stronger phase segregation.

References and Notes

(1) Finkelmann, H.; Rehage, G. In *Liquid Crystal Side Chain Polymer*; Finkelmann, H., Rehage, G., Eds.; Springer-Verlag: Berlin, 1984; Vol. 60/61, pp 99−172.
(2) Davis, F. J. *J. Mater. Chem.* **1993**, *3*, 551−562.
(3) Finkelmann, H.; Kock, H.-J.; Rehage, G. *Makromol. Chem., Rapid Commun.* **1981**, *2*, 317−322.
(4) Benne, I.; Semmler, K.; Finkelmann, H. *Macromol. Rapid Commun.* **1994**, *15*, 295−302.
(5) Meier, W.; Finkelmann, H. *Macromol. Rapid Commun.* **1990**, *11*, 599−605.
(6) Vallerien, S. U.; Kremer, F.; Fischer, E. W. *Makromol. Chem. Rapid Commun.* **1990**, *11*, 593−598.
(7) Hikmet, R. A. M. *Macromolecules* **1992**, *25*, 5759−5764.
(8) Mauzac, M.; Nguyen, H.-T.; Tournilhac, F.-G.; Yablonsky, S.-V. *Chem. Phys. Lett.* **1995**, *240*, 461−466.
(9) Omenat, A.; Hikmet, R. A. M.; Lub, J.; van der Sluis, P. *Macromolecules* **1996**, *29*, 6730−6736.
(10) Zentel, R.; Benalia, M. *Makromol. Chem.* **1987**, *188*, 665−674.
(11) Brehmer, M.; Zentel, R. *Macromol. Chem. Phys.* **1994**, *195*, 1891−1904.
(12) Sun, Shih-Jieh; Hsu, Keh-Ying; Chang, Teh-Chou *J. Polym. Sci., Part A: Polym. Chem.* **1995**, *33*, 787−796.
(13) Takahashi, T.; Nagata, F. *J. Macromol. Sci.−Phys.* **1991**, *B30*, 25−39.
(14) Papadimitrakopolous, Fotis; Hue, Shaw L.; MacKnight, William J. *Macromolecules* **1992**, *25*, 4671−4681.
(15) Eiichi, Akiyama; Koide, Naoyuki. *Liq. Cryst.* **1993**, *14*, 1645−1654.
(16) Heroguez, Valerie; Schappacher, Michel; Papon, Eric; Deffieux, Alain. *Polym. Bull.* **1991**, *25*, 307−314.
(17) Mori, K.; Tominga, T.; Matsui, M. *Synthesis* **1973**, 790.
(18) Mano, Joao F.; Correia, Natalia T.; Moura-Ramos, Joaquim J. *Liq. Cryst.* **1996**, *20*, 201−217.
(19) Zheng, W. Y.; Hammond, P. T. *Macromolecules* **1998**, *31*, 711−721.
(20) Blinov, L. M., Chigrinov, V. G. *Electrooptic Effects in Liquid Crystal Materials*; Springer-Verlag: New York, 1994.
(21) Noel, C.; Blumstein, A. In *Polymeric Liquid Crystals*; Noel, C., Eds.; Plenum Press: New York, 1985.
(22) Demus, D.; Richter, L. *Textures of Liquid Crystals*; VEB Deutscher Verlag fur Grundstoffindustrie: Leipzig, Germany 1978.
(23) Zheng, W. Y.; Albalak, R.; Hammond, P. T. *Macromolecules* **1998**, *31*, 2686−2689.

MA980753U